

## Polarized quantum dot emission in electrohydrodynamic jet printed photonic crystals

Gloria G. See, Lu Xu, Erick Sutanto, Andrew G. Alleyne, Ralph G. Nuzzo, and Brian T. Cunningham

Citation: [Applied Physics Letters](#) **107**, 051101 (2015); doi: 10.1063/1.4927648

View online: <http://dx.doi.org/10.1063/1.4927648>

View Table of Contents: <http://scitation.aip.org/content/aip/journal/apl/107/5?ver=pdfcov>

Published by the [AIP Publishing](#)

---

### Articles you may be interested in

[Patterned oxide semiconductor by electrohydrodynamic jet printing for transparent thin film transistors](#)

Appl. Phys. Lett. **100**, 102108 (2012); 10.1063/1.3691177

[Linear colloidal crystal arrays by electrohydrodynamic printing](#)

Appl. Phys. Lett. **93**, 133114 (2008); 10.1063/1.2990680

[Fabrication of a graded-wavelength guided-mode resonance filter photonic crystal](#)

Appl. Phys. Lett. **89**, 123113 (2006); 10.1063/1.2356695

[Optical properties of single droplet of photonic crystal assembled by ink-jet printing](#)

Appl. Phys. Lett. **86**, 241114 (2005); 10.1063/1.1949279

[APL Photonics](#)

---

A promotional banner for Applied Physics Reviews. On the left is a small image of the journal cover, which features a diagram of a photonic crystal structure. The main part of the banner has a blue background with a bright light source on the right. The text 'NEW Special Topic Sections' is prominently displayed in white. Below this, in orange, it says 'NOW ONLINE'. The specific topic, 'Lithium Niobate Properties and Applications: Reviews of Emerging Trends', is listed in white. The AIP Applied Physics Reviews logo is in the bottom right corner.

**NEW Special Topic Sections**

**NOW ONLINE**  
Lithium Niobate Properties and Applications:  
Reviews of Emerging Trends

**AIP** Applied Physics Reviews

# Polarized quantum dot emission in electrohydrodynamic jet printed photonic crystals

Gloria G. See,<sup>1</sup> Lu Xu,<sup>2</sup> Erick Sutanto,<sup>3</sup> Andrew G. Alleyne,<sup>3</sup> Ralph G. Nuzzo,<sup>2</sup> and Brian T. Cunningham<sup>1,4</sup>

<sup>1</sup>*Micro and Nanotechnology Laboratory, Department of Electrical and Computer Engineering, University of Illinois at Urbana-Champaign, 208 North Wright Street, Urbana, Illinois 61801, USA*

<sup>2</sup>*Department of Chemistry, University of Illinois at Urbana-Champaign, 600 South Mathews Avenue, Urbana, Illinois 61801, USA*

<sup>3</sup>*Mechanical Science and Engineering Department, University of Illinois at Urbana-Champaign, 154 Mechanical Engineering Building, Urbana, Illinois 61801, USA*

<sup>4</sup>*Department of Bioengineering, University of Illinois at Urbana-Champaign, 1270 Digital Computer Laboratory, MC-278, Urbana, Illinois 61801, USA*

(Received 31 March 2015; accepted 19 July 2015; published online 3 August 2015)

Tailored optical output, such as color purity and efficient optical intensity, are critical considerations for displays, particularly in mobile applications. To this end, we demonstrate a replica molded photonic crystal structure with embedded quantum dots. Electrohydrodynamic jet printing is used to control the position of the quantum dots within the device structure. This results in significantly less waste of the quantum dot material than application through drop-casting or spin coating. In addition, the targeted placement of the quantum dots minimizes any emission outside of the resonant enhancement field, which enables an  $8\times$  output enhancement and highly polarized emission from the photonic crystal structure. © 2015 AIP Publishing LLC.

[<http://dx.doi.org/10.1063/1.4927648>]

Lighting and display applications require color purity and tailored control of the optical properties of their output. For example, the directivity or diffusivity of a light source affects user comfort and the viewing angle of displays, while color purity determines display fidelity. Polarization is particularly crucial, as it affects contrast and power efficiency in many display devices, such as liquid crystal displays, which have a backlight that is immediately passed through a polarizer, and use transmittance filters to provide spectral control for the output.<sup>1</sup>

Quantum dots (QDs) have been investigated as a potential replacement for phosphors in lighting applications, and as a means to improve color rendering in light-emitting diode (LED) based lighting and display applications.<sup>2,3</sup> QDs offer good color saturation and purity, a capacity for solution-based processing and greater stability than many phosphors,<sup>2-4</sup> and these properties make them appealing for lighting<sup>5,6</sup> and display<sup>7</sup> applications.

Due to high fabrication costs, there is a significant interest in improving the performance and efficiency of QDs within devices. Embedding QDs within photonic crystals (PCs) offers a promising route towards increasing optical excitation efficiency, while simultaneously improving the emitted photon collection efficiency through PC-enhanced extraction.<sup>8-10</sup> The resonant conditions of a PC can be tuned to wavelengths ranging from the infrared<sup>11,12</sup> to the UV<sup>13</sup> through the appropriate design selection of the grating dimensions and refractive indices of the materials used. In addition, PCs can be designed to affect the polarization<sup>14</sup> and output directionality<sup>15,16</sup> of photon emitters embedded within them.

In PC slabs, resonant modes occur when specific phase matching conditions of the angle and wavelength of incident

light are met, allowing light to couple in and out of leaky guided resonance modes.<sup>17,18</sup> Light coupling to the PC excites a localized electromagnetic standing wave with significantly larger amplitude than that of the original source. Emission that occurs in the same spectral and physical region of this evanescent field region will couple to the guided modes of the PC, resulting in outcoupling along the phase matching angle. Because the transverse-electric (TE) and transverse-magnetic (TM) polarizations occur at different resonance conditions, it is also possible to use PCs as polarizers.<sup>17,19</sup>

In 1-D and 2-D PC slabs that serve as a quasi-planar device structure upon which QD-infused thin films can be readily applied, the optical coupling between PCs and QDs requires that the QDs reside within the resonant evanescent electric field volume, which decays exponentially away from the PC surface.<sup>20</sup> The evanescent field of a PC resonator extends from the PC surface and decreases to  $1/e$  of the peak value at a depth ranging from 10% to 50% of the resonant wavelength. Therefore, for QDs designed to emit in the visible part of the optical spectrum, QDs should be located within a few hundred nanometers of the PC surface if they are to experience enhanced excitation and enhanced extraction. Methods used to apply QD-doped polymer thin films to PCs must therefore be capable of producing film thicknesses in the 10–500 nm range.

For QDs embedded within the evanescent electric field region of a PC, emission is polarized along preferred orientations from the PC.<sup>21</sup> Polarized emission has been observed for QDs embedded within dielectric optical resonators as well as plasmonic structures.<sup>22,23</sup> As described previously, many types of display devices require a polarizer over the backlight that results in a loss of at least 50% of the optical

efficiency of the display.<sup>1</sup> Both liquid crystal<sup>24</sup> and LED-based<sup>25</sup> backlight displays have sought to polarize the light emission through more efficient means.

Nanoreplica polymer molding has been used to create PCs that contain QDs embedded in a UV-curable polymer thin film.<sup>8</sup> In such a structure, one approach for applying the QD-doped polymer thin film is spin-casting, which results in substantial waste of QDs, because only a small fraction of the QD/polymer material is incorporated into the resulting thin film, while the remaining material is cast into the spinner bowl lining.

Electrohydrodynamic jet (E-jet) printing is a recently developed approach for highly controlled spatial and volumetric deposition of liquids onto a variety of planar and non-planar surfaces. E-jet printing uses a voltage difference between the printing nozzle and the substrate to create consistent, high resolution printed patterns.<sup>26–28</sup> E-jet printing has been used for semiconductor fabrication,<sup>29</sup> biological sensing,<sup>30</sup> and micro-optical devices.<sup>26</sup> QD-embedded polymer structures have been fabricated with ink jet printing for display applications,<sup>31</sup> but E-jet printing is also capable of printing with multiple nozzles<sup>26,32</sup> and achieves finer resolution than ink jet printing, with features as small as 240 nm to 10  $\mu\text{m}$  and linewidths as narrow as 25 nm.<sup>27,28,33–35</sup> In this work, an uncured polymer containing a QD solution was printed over a specified region for replica molding, eliminating the wasted and unenhanced QDs in the polymer layer of a PC.

In this work, we demonstrate QD-embedded PCs fabricated through E-jet printing of a UV curable polymer onto a replica molding master and subsequent transfer to a substrate that supports the finished device structure. The QDs are placed inside the regions with the greatest electric field magnitude within the PC structure, resulting in a higher photon output than is produced without the PC structure. In addition,

the targeted placement of the QDs to be in close proximity to the PC grating minimizes any QD emission outside the resonant evanescent field volume. This enables highly polarized output emission, due to the significantly higher enhancement present for photons oriented to interact with the TM mode of the PC. The approach described and demonstrated in this work offers the potential to double the optical efficiency for display devices that utilize a polarized backlight by eliminating the optical power lost through a polarizing filter, while simultaneously providing an  $8\times$  enhancement in the QD emission output intensity.

The PC structure, shown in Figure 1(a), consists of a linear grating formed by replica molding a polymer doped with QDs. The polymer mixture is E-jet printed over a master, shown in the SEM images in Figures 1(b) and 1(c), where the grating has a pitch of  $\Lambda = 340\text{ nm}$  with a 67% duty cycle and a depth  $d = 120\text{ nm}$ . As illustrated in Figure 1(d), the printed structure is transferred to a plastic substrate, and a high refractive index layer of  $\text{TiO}_2$  ( $t = 105\text{ nm}$ ) is deposited over the surface of the polymer grating to create the periodic variation in the refractive index of the device.

The PCs were designed with the aid of electromagnetics simulation software (Lumerical FDTD) to enhance QD emission at one selected wavelength in the visible region of the spectrum ( $\lambda = 575\text{ nm}$ ). The photonic band structure was modeled and is shown in Figure 1(e) as a function of the angle and wavelength, with the TE and TM polarizations specifically identified at normal incidence. The darker bands indicate the locations of resonance conditions where the wavelength and angle are capable of coupling to the PC. The electric field intensity for both the TM and TE polarizations at  $\lambda = 575\text{ nm}$  excitation was modeled and a comparison is shown in Figure 2. The simulations show identical cross sections of the PC grating, with a  $3\times$  greater intensity for the TM polarization than the TE polarization. Additional details

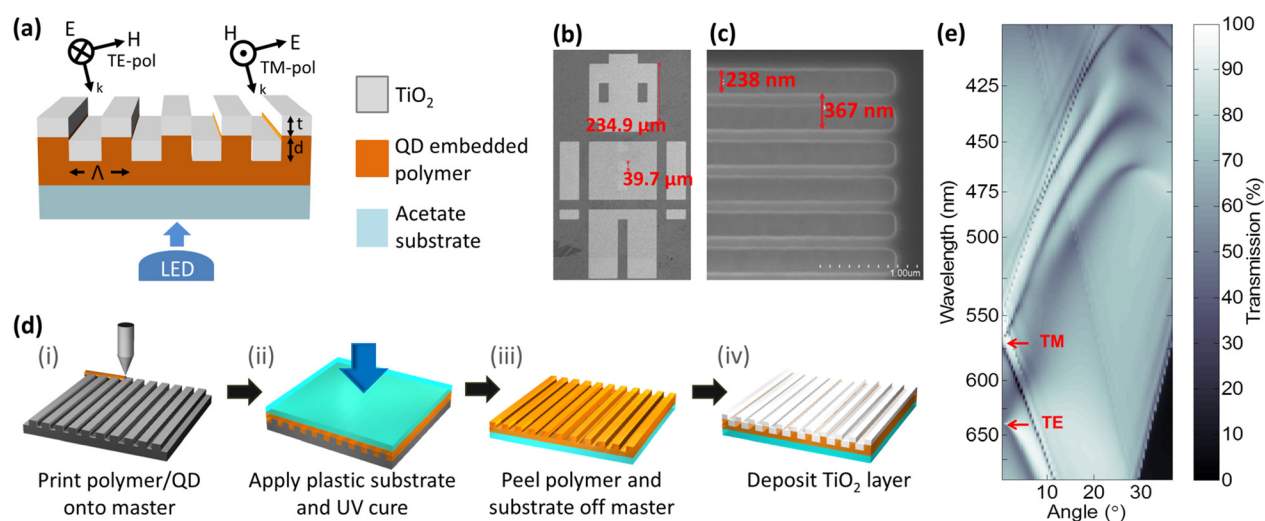


FIG. 1. (a) A schematic cross section of the device structure, consisting of a replica molded polymer layer on a flexible plastic substrate with a  $\text{TiO}_2$  film deposited over the top surface. The resulting photonic crystal has a transverse-electric (TE) polarization parallel to the linear grating, while the transverse-magnetic (TM) polarization is perpendicular to the grating. The QDs in the polymer layer are excited by collimated light from an LED. SEM images of (b) the replica molding master, from which features as small as  $40\text{ }\mu\text{m}$  were replicated with E-jet printing, and (c) the PC grating at higher magnification. (d) The PC fabrication process described in the supplementary material consists of (i) E-jet printing the QD-embedded polymer over the silicon master, (ii) applying the plastic substrate and curing the polymer, (iii) peeling off the replica from the master, and (iv) depositing the  $\text{TiO}_2$  film over the cured polymer. (e) The simulated band structure of the PC grating. The dark bands indicate the phase matching conditions for the angle and wavelength of light at which resonances occur within the PC.



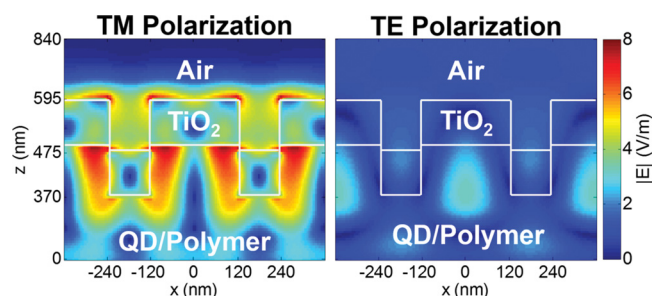


FIG. 2. Field distributions across two periods of the photonic crystal simulated using finite-difference time-domain analysis under excitation at  $\lambda = 575$  nm by TM (left) and TE (right) polarizations.

of the design and fabrication are described in the supplementary material.<sup>36</sup>

Using the testing setup described in the supplementary material,<sup>36</sup> the device was initially measured after the grating was fabricated with the QD doped polymer, but before the  $\text{TiO}_2$  deposition, to provide a baseline measurement for the output emission intensity. The measurements were repeated after the  $\text{TiO}_2$  deposition. As shown in Figure 3, at the center wavelength of  $\lambda = 575$  nm, there is an  $8\times$  enhancement in the output intensity. The inset shows a tight angular dependence of  $\pm 2.5^\circ$  for the PC enhancement at the target wavelength.

The enhanced emission is also polarized. Figure 4(a) shows the modeled and measured transmission spectra of the device. The measured transmission shows dips in the unpolarized transmission spectra occurring at wavelengths of  $\lambda = 575$  nm and 620 nm, as predicted by the model for the TM and TE modes, respectively. However, the measured transmission values are significantly larger than those predicted by the model. This is because the active device region is only 7.75% of the total substrate area that was measured, and the large inactive region contributed a significantly higher transmission to the measurement than occurs for the PC alone. The measured QD emission is shown for both the TM and TE polarizations in Figures 4(b) and 4(c), respectively, where a polarizer has been added between the device and the measurement collection optics. The TM output intensity is  $5\times$  greater than the TE, and the TE output is comparable to the noise floor of the measurement system.

The E-jet printing process allows for precise placement of QDs on the PC patterned regions, to fabricate devices that

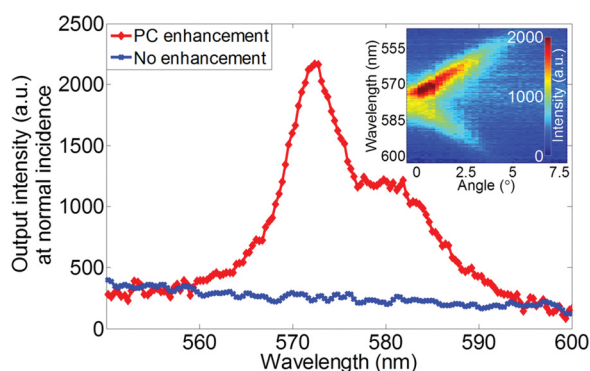


FIG. 3. An  $8\times$  enhancement in the output intensity occurs with the presence of the PC structure over the QD embedded polymer structure. The inset shows the angle dependence of the QD emission and enhancement from the PC.

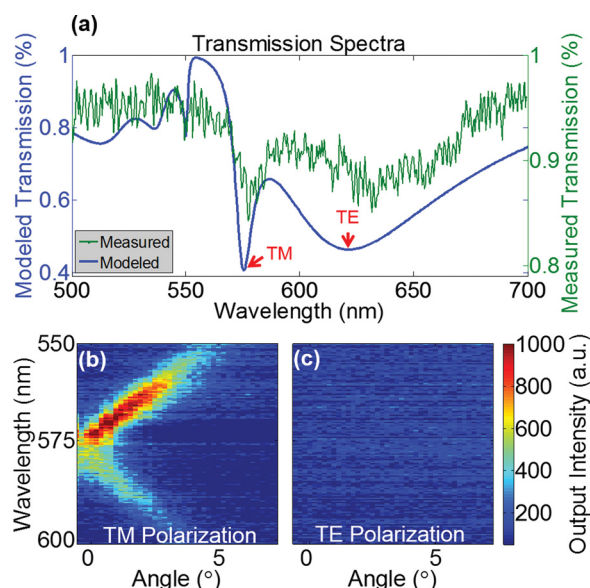


FIG. 4. (a) The modeled and measured transmission spectra of the photonic crystal at normal incidence, and the measured (b) TM and (c) TE polarized output from the PC figure. The TM polarized output demonstrates enhancement, while the output of the TE polarization is comparable to the measured background. Because the TE polarization of the PC is offset by  $\lambda = 45$  nm, there is no overlap with the TM mode, and thus no output enhancement of the QDs, creating an on/off mechanism for the QD output from the PC.

show an  $8\times$  enhancement in output intensity. This capability is important in the context of creating a surface that contains an array of PCs in the form of red-green-blue emitting pixels, where individual PC regions may be optimized for a specific wavelength of QD emitter that would be selectively printed upon them. Figure 5 shows a fluorescence microscope image of the E-jet printed device. The top inset shows the clean edges printed by the system over the device regions. The bottom inset shows a duller edge where the printing was not perfectly aligned with the PC region. The fainter regions occur where there is no PC enhancement of the QD emission and show a clearly visible contrast in brightness between the planar region and the  $8\times$  enhancement provided by the PC structure, thus verifying the enhancement effect of the PC.

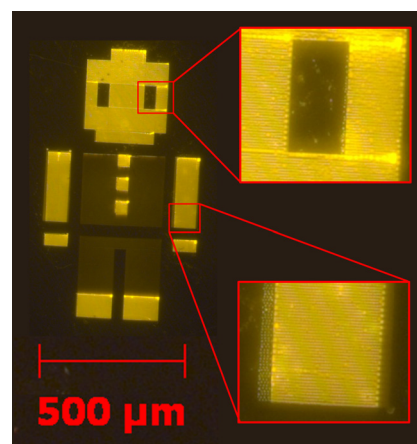


FIG. 5. A fluorescence microscope image of the E-jet printed device. The top inset shows the sharpness of the edges printed by the system. The bottom inset shows a duller edge where the printing was not perfectly aligned with the replica molding master. The fainter regions are due to QD emission occurring in a planar region with no PC structure to provide enhancement.

The cost improvements offered by the use of E-jet printing are substantial. The precise placement of the QDs eliminates the waste of spin-casting or loading QDs into device regions where there is no need for emitters. In addition, the 600 nm film thickness, compared to the 8  $\mu\text{m}$  thick layer produced with spin-casting, concentrates the emitters in the high enhancement regions of the photonic crystal and reduces the required volume of QD/polymer solution for the film by over 90%. There are minimal regions in which the QD emitters experience no enhancement and this drastically increases the total emission efficiency.

Creating initially polarized backlighting with selected color regions, as enabled by the targeted placement and polarized output of these structures, will enable significant improvements in the energy efficiency of display devices, which is critically important for displays incorporated within mobile devices. By eliminating the backlight polarizer in a display, the optical efficiency can be doubled, and eliminating color filters can triple the efficiency. These improvements are all combined with scalable production by nanoreplica molding and the use of flexible plastic substrates, which enable an array of novel device platforms.

Future improvements for the devices include the use of QDs that can be excited with a non-UV source. In addition, increasing the printing speeds and printing red-green-blue specific device regions would improve the viability for scalable display production. If coupled with thin film transistors for switching, then E-jet printed PC regions would provide pixelated control of color and polarization for use in screen displays for computers, televisions, and other devices that require the high color purity of QDs.

The devices in this work demonstrate the precise placement of QDs within specific regions of replica molded PCs, using a scalable fabrication method. The devices show both polarized emission and an  $8\times$  increase in output intensity, as compared to output emission without the PC structure. These improvements have the potential to eliminate polarizers from backlight display technology and double their optical efficiency. The E-jet fabrication methodology decreases the wasted QD material by more than 90% from spin- and drop-casting techniques for identical device areas through the controlled placement of QDs. These cost and performance improvements are key advances toward overcoming the barriers to cost-effective QD display technology.

The authors are grateful for the support of Dow Chemical Company under Research Agreement No. 226772AC.

<sup>1</sup>M. Suzuki, in Soc. Inf. Disp. Conf., Los Angeles (2011).

<sup>2</sup>D. V. Talapin and J. Steckel, *MRS Bull.* **38**, 685 (2013).

<sup>3</sup>H. S. Jang, H. Yang, S. W. Kim, J. Y. Han, S.-G. Lee, and D. Y. Jeon, *Adv. Mater.* **20**, 2696 (2008).

<sup>4</sup>H.-F. Xiang, S.-C. Yu, C.-M. Che, and P. T. Lai, *Appl. Phys. Lett.* **83**, 1518 (2003).

<sup>5</sup>K.-S. Cho, E. K. Lee, W.-J. Joo, E. Jang, T.-H. Kim, S. J. Lee, S.-J. Kwon, J. Y. Han, B.-K. Kim, B. L. Choi, and J. M. Kim, *Nat. Photonics* **3**, 341 (2009).

<sup>6</sup>W. K. Bae, S. Brovelli, and V. I. Klimov, *MRS Bull.* **38**, 721 (2013).

<sup>7</sup>G. J. Supran, Y. Shirasaki, K. W. Song, J. Caruge, P. T. Kazlas, S. Coe-sullivan, T. L. Andrew, M. G. Bawendi, and V. Bulovi, *MRS Bull.* **38**, 703 (2013).

<sup>8</sup>F. Yang and B. T. Cunningham, *Opt. Express* **19**, 3908 (2011).

<sup>9</sup>L. Petti, M. Rippa, J. Zhou, L. Manna, M. Zanella, and P. Mornile, *Nanoscale Res. Lett.* **6**, 371 (2011).

<sup>10</sup>M. R. Singh, C. Racknor, and D. Schindel, *Appl. Phys. Lett.* **101**, 051115 (2012).

<sup>11</sup>L. Chen, W. Zhou, Z. Qiang, and G. J. Brown, *Proc SPIE* **6370**, 637011 (2006).

<sup>12</sup>I. D. Block, N. Ganesh, M. Lu, B. T. Cunningham, and S. Member, *IEEE Sens. J.* **8**, 274 (2008).

<sup>13</sup>N. Ganesh and B. T. Cunningham, *Appl. Phys. Lett.* **88**, 071110 (2006).

<sup>14</sup>J. Rosenberg, R. V. Shenoi, S. Krishna, and O. Painter, *Opt. Express* **18**, 3672 (2010).

<sup>15</sup>M. Barth, A. Gruber, and F. Cichos, *Phys. Rev. B* **72**, 085129 (2005).

<sup>16</sup>C. Wiesmann, K. Bergenek, N. Linder, and U. T. Schwarz, *Laser Photonics Rev.* **3**, 262 (2009).

<sup>17</sup>R. Magnusson and S. S. Wang, *Appl. Phys. Lett.* **61**, 1022 (1992).

<sup>18</sup>S. S. Wang and R. Magnusson, *Appl. Optics* **32**, 2606–2613 (1993).

<sup>19</sup>S. S. Wang, R. Magnusson, and J. S. Bagby, *J. Opt. Soc. Am. A* **7**, 1470 (1990).

<sup>20</sup>N. Ganesh, P. C. Mathias, W. Zhang, and B. T. Cunningham, *J. Appl. Phys.* **103**, 083104 (2008).

<sup>21</sup>R. Oulton, B. D. Jones, S. Lam, A. R. a. Chalcraft, D. Szymanski, D. O'Brien, T. F. Krauss, D. Sanvitto, A. M. Fox, D. M. Whittaker, M. Hopkinson, and M. S. Skolnick, *Opt. Express* **15**, 17221 (2007).

<sup>22</sup>G. Lozano, D. J. Louwers, S. R. K. Rodriguez, S. Murai, O. T. A. Jansen, M. A. Verschuuren, and J. G. Rivas, *Light: Sci. Appl.* **2**, e66 (2013).

<sup>23</sup>S. R. K. Rodriguez, G. Lozano, M. A. Verschuuren, R. Gomes, K. Lambert, B. De Geyter, A. Hassinen, D. Van Thourhout, Z. Hens, and J. G. Rivas, *Appl. Phys. Lett.* **100**, 111103 (2012).

<sup>24</sup>P. Yao, C. Chung, C. Wu, and C. Chen, *Opt. Express* **20**, 4819 (2012).

<sup>25</sup>H. Masui, N. N. Fellows, S. Nakamura, and S. P. DenBaars, *Semicond. Sci. Technol.* **23**, 072001 (2008).

<sup>26</sup>E. Sutanto, Y. Tan, M. S. Onses, B. T. Cunningham, and A. G. Alleyne, *Manuf. Lett.* **2**, 4 (2014).

<sup>27</sup>J.-U. Park, M. Hardy, S. J. Kang, K. Barton, K. Adair, D. K. Mukhopadhyay, C. Y. Lee, M. S. Strano, A. G. Alleyne, J. G. Georgiadis, P. M. Ferreira, and J. a. Rogers, *Nat. Mater.* **6**, 782 (2007).

<sup>28</sup>S. Mishra, K. L. Barton, A. G. Alleyne, P. M. Ferreira, and J. A. Rogers, *J. Micromech. Microeng.* **20**, 095026 (2010).

<sup>29</sup>M. S. Onses, C. Song, L. Williamson, E. Sutanto, P. M. Ferreira, A. G. Alleyne, P. F. Nealey, H. Ahn, and J. A. Rogers, *Nat. Nanotechnol.* **8**, 667 (2013).

<sup>30</sup>K. Shigeta, Y. He, E. Sutanto, S. Kang, A. Le, R. G. Nuzzo, A. G. Alleyne, P. M. Ferreira, Y. Lu, and J. A. Rogers, *Anal. Chem.* **84**, 10012–10018 (2012).

<sup>31</sup>B. V. Wood, M. J. Panzer, J. Chen, M. S. Bradley, J. E. Halpert, M. G. Bawendi, and V. Bulovic, *Adv. Mater.* **21**, 2151 (2009).

<sup>32</sup>A. Khan, K. Rahman, D. Soo, and K. Hyun, *J. Mater. Process. Technol.* **212**, 700 (2012).

<sup>33</sup>E. Sutanto, K. Shigeta, Y. K. Kim, P. G. Graf, D. J. Hoelzle, K. L. Barton, A. G. Alleyne, P. M. Ferreira, and J. A. Rogers, *J. Micromech. Microeng.* **22**, 045008 (2012).

<sup>34</sup>K. Barton, S. Mishra, K. A. Shorter, A. Alleyne, P. Ferreira, and J. Rogers, *Mechatronics* **20**, 611 (2010).

<sup>35</sup>B. H. Kim, M. S. Onses, J. Bin Lim, S. Nam, N. Oh, H. Kim, K. J. Yu, J. W. Lee, J.-H. Kim, S.-K. Kang, C. H. Lee, J. Lee, J. H. Shin, N. H. Kim, C. Leal, M. Shim, and J. a. Rogers, *Nano Lett.* **15**, 969 (2015).

<sup>36</sup>See supplementary material at <http://dx.doi.org/10.1063/1.4927648> for additional details of the device fabrication, design, and testing.